Chapter 1

Structure of Complex Materials

Chapter Outline

1.1. CRYSTALLOGRAPHY AND BEYOND

1.1.1. Complexity at the Atomic and Molecular Level

Mankind faces some daunting technological challenges inc the twenty-first century. With world population growing above 10 billion and countries undergoing rapid economic development, and therefore increasing their energy intensity (the energy use per person), there is enormous pressure on energy, food, and water resources, with serious impacts also on the environment

Pergamon Materials Series, Vol. 16. http://dx.doi.org/10.1016/B978-0-08-097133-9.00001-0

through pollution and climate change. It will be imperative to switch to sustainable energy sources, while simultaneously expanding the food and fresh water supplies. The roadblock to most of these next-generation technologies are materials. Batteries need to have higher energy densities while being cheaper, safer, and better for the environment; fuel cells need to be cost-effective; photovoltaics need to have higher conversion efficiencies while being cheap and environmentally benign; catalysts are sought for splitting of water directly from sunlight; and so on. Advanced materials are required for all these applications, and increasingly we are looking at materials that are complex, nanostructured, and often heterogeneous. For example, nanoparticles in photovoltaics supported nanoparticles as catalysts in fuel-cell electrodes, which are themselves highly disordered and nanostructured and formed into micron-scale heterogeneous packages with electrodes, membranes, and electrolytes. Materials science holds the key to these next-generation technologies, but we are now required to work at the extreme frontier of complexity.

For a long time, complexity has been a bad word for scientists. Simplicity has been the preferred choice, and pronouncing a problem complex was an artful way of giving up any attempt to find a solution. However, major changes are taking place today, placing complexity at the forefront of research in various fields including materials research. Historically, the first materials humankind used were complex materials made by nature, such as wood and animal bones. But after they discovered the art of extracting pure materials such as copper and iron, simple materials started to prevail. This tendency was greatly accelerated during the industrial revolution that enabled production of simple materials in abundance at a low cost.

However, complex materials are on the comeback, as in recent years technological progress made it possible to produce man-made complex materials with superior properties. Composites such as graphite–boron are used in all kinds of sporting equipment from golf shafts to tennis rackets. Multilayered thin films are used in magnetic heads of disk memories, and computer chips are very complex heterogeneous constructs of silicon oxide, films and metal interconnects. While many of these artificial structures are composed of relatively simple materials built into a complex structure, other materials are atomistically complex. Many of the modern electronic materials that exhibit remarkable properties, such as high-temperature superconductivity, colossal magnetoresistivity, or high dielectric or thermoelectric response, have intrinsically complex atomic and nanoscale structures that appear to be critically important to their performance. Polymers are structurally highly complex, with millions of atoms constituting chain molecules, which are assembled in a complex morphology, partly crystalline and partly amorphous. Humankind has started with complex natural materials, developed civilization with simple man-made materials, and is now moving forward to close the circle with man-made complex materials.

However, while polymers are in many ways similar to biological materials, they are still much simpler than proteins. Biological protein molecules are enormously complex; they self-organize with their unique ways of folding up. The functionality of a living organism comes from a multitude of folded proteins, each with a very precise and unique function. For example, the enzyme desaturase is found in plants. It has the job of desaturating fat molecules used in the plant's cell walls in order to maintain their flexibility when the weather gets cold. It does nothing else but its unique, directed, function is of critical importance to the survival of the plant. There is a clear universal trend; the more directed the functionality of a material, the greater its structural complexity. To harness this law to our benefit in future man-made materials, it is clearly necessary to have control over complex structures and to be able to characterize them in detail.

1.1.2. Local View of the Structure

One of the major reasons why nanoscale structural complexity is important to advanced functional materials is that solids which contain competing internal forces are often highly sensitive, and these forces result in a complex structure. If two or more forces are competing against each other, the balance can be tipped by a small external force and the system responds with vigor. An example is the colossal magnetoresistive (CMR) oxides which have recently been studied extensively. The CMR materials are located in the phase diagram right at a metal-to-insulator (MI) transition, and an applied magnetic field greatly increases their conductivity by inducing a transition from an insulator to a metal. In these materials, there are forces that are competing to localize and delocalize charge carriers, and they are balanced right at the MI transition. A magnetic field helps the delocalizing force and propels the system into the metallic state.

Such competition usually produces a complex structure. The competition can be manipulated by changing composition, temperature, as well as the nanoscale structure. For example, to induce the MI transition at a particular temperature, the charge density in the material is adjusted chemically by randomly substituting one element for another. When there are competing forces at the atomic scale, the structure will reflect the conflict, for instance, by introducing a slight distortion. If this occurs in a random alloy, the distortion will vary from one atomic site to the next, resulting in a highly aperiodic structure with nanoscale variations. As will be discussed later in this book as an example, the CMR oxides are made up of nanoscale regions of insulating and metallic domains, each having a slightly different local distortion in the structure. In addition, these regions are not necessarily static but could be moving dynamically. Therefore, we have to consider not only various length scales but also various timescales. However, as these dynamics are usually not accessible by X-ray scattering, in this book, we focus mainly on the

static or instantaneous structure, and only one chapter will be devoted to the dynamic phenomena observed by neutron inelastic scattering.

As a result of such competition, these complex materials have a structure that locally deviates from the perfect crystal structure, even when they may appear superficially crystalline. In real life as well, a complex person is always more interesting than a simple one, as such a person is unpredictable. A perfectly periodic crystal may be beautiful in some sense, but is totally predictable and can be extremely boring; even the most beautiful theme of Mozart would become boring if it were repeated a million times! Modern complex materials, on the other hand, are far from boring.

In studying such complex crystals with local deviations, we need to take two distinct points of view. One is a global view and the other is a local view. They are like national statistics and personal reports in describing an event such as a war between nations. The death tolls are certainly needed to grasp the scale and economic impact of the war, but novels such as *War and Peace*, *All Quiet on the Western Front*, *For Whom the Bell Tolls*, or even *Gone with the Wind* tell us more vividly what really happened at a human level and what the war meant to individual people. The average structure determined by crystallography presents a global view of the structure. However, as the real interactions are taking place at a local level, they are more directly related to the local structure, which can only be studied by local probes. In the case of well-ordered crystals, the distinction is irrelevant. The global structure also reveals the local structure. However, as we describe in this book, this is no longer the case when local distortions are present in which case the local structure must be studied directly in conjunction with the global structure.

This distinction has a direct implication for the method of theoretical analysis as well. The global view in this case corresponds to the simple mean-field approximation (MFA), in which numerous competing forces are volume-averaged into two or more representative competing forces. The conflict is then assessed at a global scale. However, in a complex, nonlinear system, the conflict often remains local. In order to describe such local conflicts, the average structure is nearly meaningless, and we have to know the precise local structure where the conflicts take place.

The problem of competing forces in complex systems has interesting political and sociological analogies. G.W.F. Hegel (1770–1831) was probably the first European philosopher who recognized the dynamic and creative effect of competition. Marxism has the Hegelian philosophy as its basis, but in its application, the complex sociological competition was abstracted as the struggle between two social classes. This is the philosophical equivalent of taking the MFA. An irony of this is that, in the implementation of Marxism in the communist societies of the twentieth century, competition was essentially eliminated. In large part, this was at the root of the demise of communism, as competition is the vital force that drives development, as Hegel originally pointed out. In materials, the competition between comparable forces gives

rise to dynamic and interesting effects. These effects are primarily local, varying sharply from atom to atom. As in the case of Marxism, taking the MFA and considering only the global effects may mask the important underlying local physics. In this case, a study of complex competing forces in solids has to start at a local level. The condition of balance between competing forces should be evaluated locally rather than globally, just like voting to elect local representatives in a democracy. The macroscopic properties are determined as a consequence of interactive accumulation of local properties. That is why the study of local structure is ever more important in understanding complex structures containing competing interactions.

Depending on the length scale of the complexity, different tools are required to investigate the state of such complex structures. As we focus on complexity in the structure at the atomic to nanometer ($10^{-9\sim10}$ m) scale, the methods to use are X-ray, neutron and electron diffraction techniques, as well as computer modeling. However, the regular crystallographic methods of structural analysis are not going to be sufficient in studying these complex materials, as the crystallographic method *a priori* assumes perfect lattice periodicity. Actually, strictly speaking, even a perfect crystal is not truly periodic because of quantum-mechanical and thermal vibrations. If one takes a snapshot of the structure, the crystal symmetry is gone, including the translational symmetry. As we will discuss later, in the case of harmonic lattice vibrations, the Debye–Waller approximation does an excellent job of recovering the symmetry. However, in complex structures, the Debye–Waller approximation usually fails, and we have to determine local structural details by using a different approach. Another philosophical point is that we have to accept a probabilistic description, rather than a deterministic description, to describe the structure. For a perfect crystal, translational symmetry works the miracle of Bragg's law and reduces the number of parameters to describe the structure to a precious few. In complex materials, the structure is often described in terms of probabilities and parameters to specify these probabilities.

Both of these points suggest that some fundamental departures from crystallography are required to know the true structure of complex materials. However, we are creatures of habit, and too often we rely upon crystallography to describe the structure of materials, no matter how complex they are. In this book, we first discuss how dangerous such a practice is, introduce alternative local tools of structural study, and go over several examples to illustrate the purpose of the local structural study. Reflecting the two philosophical points mentioned above in our new approach, we will not assume periodicity, and the structure will be described statistically. Another important component in the study of complex materials is imaging, for example, using transmission electron microscopy or, increasingly, these days using intense X-ray beams. This is a huge topic that is dealt with well in other books, and we do not discuss it in any great detail here.

1.1.3. Shadow of Bragg's Law: Why Knowing the Crystal Structure Is Not Sufficient

Bragg's law is the foundation of crystallography, one of the first subjects that an undergraduate student in materials science or condensed matter physics learns in class. It is the basis for crystallography that has revolutionized our view of the world since its discovery around 100 years ago. At that time, the very existence of atoms was still somewhat controversial, but it soon became possible to reveal their microscopic arrangement in materials. After extensive development both theoretically and experimentally over the intervening years, crystallography can now routinely determine the arrangement of proteins with many thousands of unique atoms in the unit cell: A truly remarkable achievement. However, a prerequisite for Bragg's law is the periodicity of the structure. The material has to be a crystal to do crystallography. When the particle size of the material gets very small, as is the case for small nanoparticles, or when structural order exists that extends only over a few nanometers within a bulk material, Bragg's law stops working. This is the so-called nanostructure problem (Billinge 2010; Billinge and Levin, 2007). We do not have robust, quantitative methods for solving structure at the nanoscale; the nanoscale replacement for crystallography. The pair density function (PDF) is a powerful approach that yields structural information at the nanoscale and has been used for nanostructure solution as we describe later in the book (Juhás *et al*., 2006), but it is still far from routine. This is still an active area of research of which PDF is just one branch. A broader discussion of this issue is beyond the scope of this book, but the problem is laid out in Billinge and Levin (2007).

Bragg's law is so basic and taken so completely for granted that we tend to forget how powerful this law really is. However, it is a truly mighty magic wand. One way of describing the atomic structure of a material is to specify the position of each atom. But if a piece of crystal has 10^{23} atoms, in order to specify the position of these atoms, one would need 3×10^{23} numbers describing the x, y, and z coordinates of each atom. If one goes about determining these positions atom by atom, it will take forever to accomplish such a task. However, by using Bragg's law based upon the translational symmetry, these 3×10^{23} numbers can be reduced to a small set of numbers specifying the lattice symmetry and atomic positions within the unit cell.

Also by applying Bragg's law, the lattice constant can be determined routinely with accuracy exceeding 10^{-5} Å. This is, however, an amazing feat, as usually to measure a length with such accuracy requires the use of a probe with a comparable wavelength ($\lambda = 10^{-5}$ Å). If we use a gamma ray, its energy must be over 1 GeV, and if we use an electron, the energy necessary is over 40 GeV. In either case, one has to use major particle accelerators costing billions of dollars to produce probes with such energy. But with the use of Bragg's law, this is achieved with a small, inexpensive, 50-keV X-ray generator. It is indeed magic.

The secret to this magic can be uncovered by going back to basics. As the success of Bragg's law has been so spectacular, we tend to forget that the crucial presumption for Bragg's law is the periodicity of the crystal lattice. Because of the translational symmetry, the description of the crystal structure is reduced to specifying the symmetry group and one or a few lattice parameters, a, b, and c. However, by the diffraction measurement, we actually measure not the lattice constant but the lattice coherence length, $\xi = Na$. If the uncertainty in ξ is λ, the uncertainty in a is λ/N, which can easily be as small as 10^{-5} Å if $\lambda = 1$ Å and $N = 10^5$.

The lattice periodicity is crucial to the success of Bragg's law. If the structure of a crystal is not perfectly periodic, we cannot reap the benefit of Bragg's law and we then have to face the unpleasant reality of describing the structure in other ways. Again, trying to determine all the atomic positions is out of the question. If the deviations from perfect crystallinity are small in number, the concept of lattice defects is often useful. Also, if the deviations are smoothly varying in space, they may be described by elasticity theory. Several methods have been developed in crystallography to deal with limited amounts of disorder, as we will discuss in Chapter 2. However, in some cases, the deviations are so pervasive that neither of these concepts and remedial methods are sufficient. A more pertinent approach is to leave the familiar protection of Bragg's law behind and directly face the complex and unfamiliar reality. The precedent for this kind of study is found in the research field of noncrystalline materials.

1.1.4. The Methods of Local Crystallography

Glasses and liquids have no structural periodicity, and yet their atomic structure is not altogether random as in gases. What does it mean, then, to know the structure? Specifying all the atomic positions is not only impractical but also useless. Even if we were given a huge table of numbers containing 3×10^{23} atomic coordinates, we would be completely overwhelmed and would not be able to comprehend and use such information. The amount of information is simply too big. Intelligence, on the other hand, means the capability to select the essential pieces out of a vast sea of information, and to reorganize them into a new meaningful statement called understanding. As we go through our lives, we experience a huge number of events. Experiences themselves, however, would not make us wise. Only after reflecting upon the experience and deducing the essential message from these experiences, do we learn something from life.

The purpose of structural analysis is to relate the structure to the properties so that we can understand the properties from the atomistic point of view. This understanding can lead to improvement of the material or creation of new ones with better properties. Clearly, the properties are not determined by the absolute position of each atom, but by the relative positions of the

atoms which are close enough to have some interaction. In other words, local atomic environment, the relative positions of the near-neighbor atoms, is what we have to know in deliberating about the properties of the material. From this point of view, the crystal symmetry, so highly revered in the world of crystallography, may not be as important as is often portrayed. If the distortion that breaks the symmetry is extremely small, the effect on the properties may be very small, even if, strictly speaking, the symmetry is altered. On the other hand, large aperiodic local displacements of atoms usually have serious consequences on the properties, even when they do not change the average symmetry.

The relative atomic positions, or the interatomic positional correlations, can be described by a set of interatomic distances, $r_{\nu\mu}$, where ν and μ refer to the individual atoms. If the system is macroscopically isotropic, as in liquids, the distribution of the interatomic distances is given by

$$\rho(r) = \rho_0 g(r) = \frac{1}{4\pi N r^2} \sum_{\nu} \sum_{\mu} \delta\left(r - r_{\nu\mu}\right), \tag{1.1}$$

where ρ_0 is the number density of atoms in the system of N atoms. The δ is a Dirac delta function. The function $\rho(r)$ is called the atomic PDF. The function $g(r)$ is called the atomic pair distribution function, also abbreviated as PDF. The PDF is a one-dimensional function which has peaks at distances, $r_{\nu\mu} = |\mathbf{r}_\nu - \mathbf{r}_\mu|$, separating the νth and μth atoms. The sums are taken over all the atoms in the sample. What results is a histogram of all the atom–atom distances in the solid. In practice, there are so many atoms in the material that $\rho(r)$ becomes a quasicontinuous distribution function. An example of a PDF for an amorphous metallic alloy is shown in Fig. 1.1. Note that $\rho(r) = \rho_0 g(r)$ is practically zero below a certain value of r, as two atoms cannot come too close to each other. There is a large peak at the average atomic separation, usually 2–3 Å, representing the nearest neighbors, and there are some oscillations beyond the first peak due to short-range order.

In this example of a material with no long-range order, $\rho(r)$ asymptotes to the value of ρ_0 at high-r (note that $g(r)$ asymptotes to 1). At low-r, ρ(r) oscillates up and down above and below the average density. These oscillations contain the useful local structural information. Because we are measuring deviations from the average density, these oscillations are referred to as "correlations," and $\rho(r)$ and $g(r)$ are often called "pair correlation functions." They give information about correlations (deviations from average behavior) of pairs of atoms.

From these functions, one can learn various pieces of information regarding the local environment of atoms, such as how many neighbors there are and how far away they are. While the PDF provides only one-dimensional information, it is possible to recreate the three-dimensional structure by creating a three-dimensional model, the PDF of which agrees with the experimental

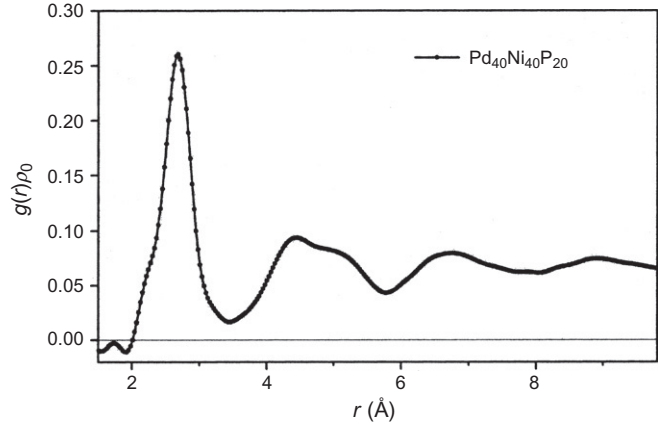

FIGURE 1.1 The atomic PDF, $\rho(r) = \rho_0 g(r)$, from the amorphous metallic alloy $Pd_{40}Ni_{40}P_{20}$ showing the generic behavior of $g(r)$ for an amorphous material. The data asymptote to zero at low-r and to $\rho_0 = 0.07$ Å^{-3} at high-r equivalent to $g(r) = 1$. In-between, the PDF oscillates showing atomic correlations (deviations from the average density), for example, a greater probability of finding an atom at the hard-sphere separation distance of 2.9 Å, followed by a less than average probability of finding a neighbor between the first and second neighbor shell at 3.5 Å, and so on (Egami *et al.*, 1998).

PDF (Chapter 6). In principle, the approximation of an isotropic sample can be removed, and the extension of the equations to define three-dimensional distribution functions is treated in Chapter 3.

The PDF can be experimentally determined by diffraction measurements using X-rays, neutrons, or electrons, as discussed in Chapter 4, or by the method of X-ray absorption fine structure (EXAFS). The EXAFS method is not the focus of this book; however, for completeness, a discussion of this technique, and its relationship to diffraction techniques, is given in Appendix 3.4. These methods of structural study are applicable for any system, amorphous or crystalline, isotropic or anisotropic, and powder or single crystal. In this book, we mainly deal with the PDF determined by powder diffraction. Powder diffraction experiments are the simplest measurements and, in many cases, provide enough relevant information to understand the phenomena of interest.

While the PDF method is an established technique in the field of structural study of glasses and liquids until recently it has hardly been used for the study of crystalline solids. There are two reasons for this lack of activity. The primary reason is that technology was not ready. If one uses X-rays from the regular sealed X-ray tube in the laboratory or thermal neutrons from a nuclear reactor as radiation, the wavelength of the radiation is too long for the PDF to be determined accurately and with high resolution, as we discuss later. Also, obtaining kinematical scattering that can yield accurate PDFs with electrons is

tricky and required the development of two-dimensional CCD detectors and data analysis developments. The advent of synchrotron-based radiation sources, such as pulsed spallation neutron sources and X-ray synchrotron sources, that provide high-intensity short-wavelength particles has made the PDF method accurate and reliable. The secondary reason is that, with these techniques, data analysis and modeling is highly computationally intensive and has only become practical with the recent advent of high-speed computing. Finally, as we mentioned above, the need for studying the detailed atomic structure of complex materials is relatively new, instigated by the discovery of such materials.

Many of the subjects discussed in this book are dealt with in a number of standard textbooks listed in the bibliography. However, due to advances in facilities, equipment, experimental techniques, and modeling, it is worthwhile to cast a new light on the subjects. In particular, the application of the PDF method for the structural study of crystalline solids is outside the scope of these classical books, while that is the main focus of the present book, with recent results being used as examples of application.

1.1.5. Real and Reciprocal Space

Diffraction methods measure diffracted intensity as a function of the momentum transfer of the scattering particle, $\mathbf{Q}$, which is defined as $\mathbf{Q} = \mathbf{k}_{\text{init}} - \mathbf{k}_{\text{final}}$, where $\mathbf{k}_{\text{init}}$ and $\mathbf{k}_{\text{final}}$ are the incident and scattered wavevectors, respectively. For this reason, $\mathbf{Q}$ is also called the diffraction vector. The data naturally appear in the so-called reciprocal space as intensity as a function of wavevector. Clearly, from the definition of $\rho(r)$, this function is a direct representation of the real structure and exists in real space as a function of position. These two domains are linked by a Fourier transform, as we discuss in detail later. However, it becomes immediately apparent that the same information about the local structure can be equally well represented in either real or reciprocal space. The reciprocal space equivalent of $\rho(r)$ is $S(Q)$, the total scattering structure function.[1]

The name "total scattering" comes from the fact that included in the intensity is scattering coming from Bragg peaks (the global structure), elastic diffuse scattering (the static local structure), and inelastic diffuse scattering from moving atoms that contains information about atom dynamics, all measured over a wide range of Q such that *all* (or as much as possible) of the coherent scattering is collected. As these intensities are not resolved and differentiated,

1. $S(Q)$ is widely referred to as the structure factor in the world of noncrystalline materials. This is an unfortunate misnomer and causes confusion when these ideas are introduced to crystallographers who have their own, quite distinct and appropriately named, crystallographic structure factor, F_{hkl}. We prefer to call $S(Q)$ the total scattering structure function, as it is a continuous function of intensity versus Q and not a factor that scales a Bragg peak amplitude as in the case of F_{hkl}.

the resultant scattering intensity is referred to as total scattering. The study of local structure described in this book generically comes down to the study of the total scattering intensity, $S(Q)$. This can be studied directly in reciprocal space or by Fourier transforming to real space and studying the PDF. Both approaches are valid and tend to provide complementary information. Examples of both approaches are described in this book, though the emphasis is on the study of the PDF, as this is the particular expertise of the authors.

1.2. THE POWER OF TOTAL SCATTERING AND PDF METHODS

Before we submerge ourselves into the details of the diffraction physics and the PDF method, let us quickly review some examples that illustrate the power of the PDF and total scattering methods. Details regarding each example will be expanded upon later in the book. However, these brief descriptions should help the reader to have some concrete images of what we are talking about and also will hopefully motivate the reader to read further.

1.2.1. The Difference Between the Local and Average Structures: Alloys

What exactly is meant by the difference between the local structure and the average crystallographic structure? A simple example is found in the case of an alloy semiconductor. Semiconductors Ga–As and In–As have the same structure but different band gaps; the band gap can be engineered by alloying them to form a pseudo-binary compound $(Ga_{1-x}In_x)As$. The lattice constant changes approximately linearly with x, following Vegard's law. Crystallographically then, the distance between the (Ga,In) site and the As site changes linearly with x. This, however, does not mean that actual bond length changes linearly with x. We know that a large energy is needed to change the bond length, and it is most likely that the Ga–As distances and the In–As distances endeavor to remain more or less constant even when x is changed. In this covalent solid, the structural disorder due to the alloying is predominantly relaxed by bond bending that requires relatively less energy.

The crystallographic (Ga,In)–As distance represents only the average distance between the atoms at the (Ga,In) and As sites, and corresponds to neither the actual Ga–As nor In–As distances. When x is changed the number of Ga—As and In—As bonds changes linearly with x, resulting in the linear change in the average lattice constant. Crystallography gives you only the average bond distance and the lattice constant and does not tell you the actual local bond length. In order to determine the local bond, one requires local probes.

Indeed, the PDF determined by high-energy X-ray diffraction clearly shows that the nearest-neighbor (Ga,In)–As peak at $\sim$0.4 Å is split into two subpeaks, as shown in Fig. 1.2 (Petkov *et al.*, 1999). The dependence of

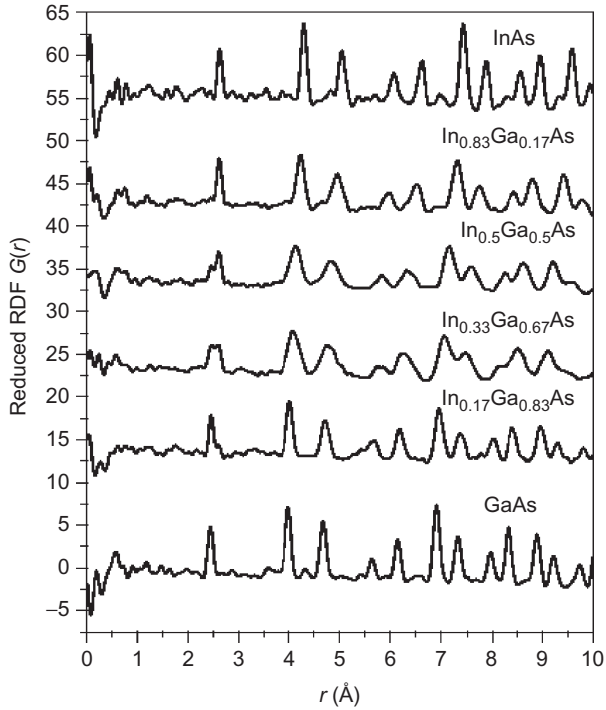

FIGURE 1.2 PDFs in the form $G(r) = 4pr(r(r) - r_0)$ from $In_{1-x}Ga_xAs$ alloys. Data were measured from high-energy X-ray diffraction data at Cornell High Energy Synchrotron Source (CHESS) at 10 K. Notice the first peak is split indicating the presence of short Ga—As and a long In—As bonds (Jeong *et al*., 2001; Petkov *et al*., 1999).

the positions of the subpeaks on composition x is shown in Fig. 1.3. The subpeak positions connect smoothly to the Ga–As and In–As distances in the pure compounds, revealing the chemical identity of these peaks.[2]

A weak dependence of the peak position on x means that the size mismatch leads to a small amount of local atomic-level strain (Egami and Aur, 1987; Eshelby, 1956).

1.2.2. Short- Versus Long-Range Correlations: Molecular Solids

Another example that illustrates the notion of local versus global structure is a molecular solid, for instance, a crystal of C_{60} or buckyballs (Fig. 1.4a). Buckyballs form an f.c.c. solid (Fig. 1.4b). At and above room temperature, each molecule is randomly rotating. Thus, the time-averaged structure is just

2. This behavior was first seen in another local technique, EXAFS (Mikkelson and Boyce, 1982); however, the PDF study reveals the intermediate range order and gives a more complete structural solution.

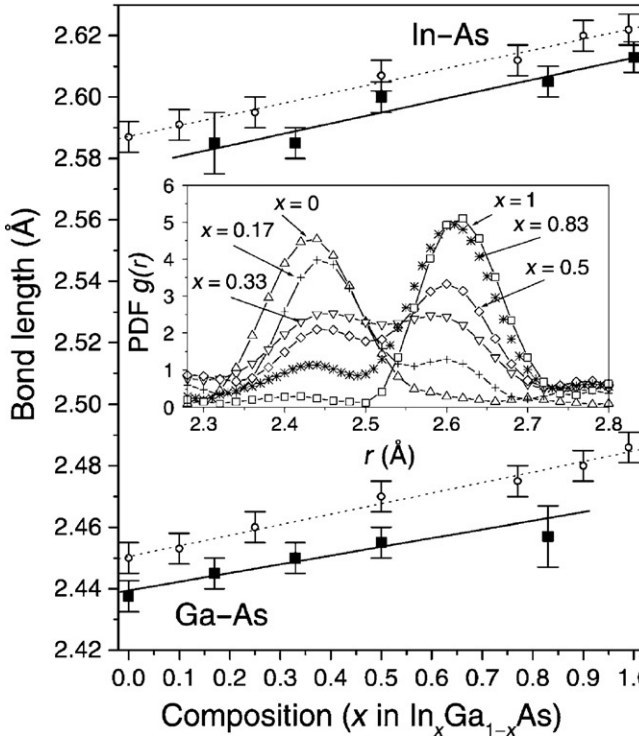

FIGURE 1.3 The dependence of the lengths of the short and long bonds in $In_{1-x}Ga_xAs$ alloys as a function of doping. The inset shows a close-up of the PDF of the near-neighbor In/Ga—As bonds for various compositions with model predictions superimposed (Petkov *et al*., 1999).

an f.c.c. structure of uniform hollow balls with the diameter of about 7 Å. However, within each buckyball, the network of carbon atoms is rigid. Translated into the language of the PDF, this means that the carbon atoms within the same buckyball are highly correlated, but those on different buckyballs are not correlated. Thus, as shown in Fig. 1.4d, the PDF exhibits sharp features up to 7 Å which is the diameter of the buckyball, reflecting the discrete interatomic distances within the molecule, while it becomes a slowly varying function beyond, without atomic details.

The broad peaks in the PDF beyond 7 Å are real and come from the f.c.c. arrangement of isotropic spherical balls. The nearest-neighbor ball–ball separation, a, is $\sim$10 Å corresponding to the first broad peak. The second and third neighbors are at $\sqrt{2}a$ and $\sqrt{3}a$, that is, $\sim$14 and $\sim$17 Å, as observed.

This shows that, within the same PDF, different information about the local structure (intra- and interdomain correlations) is contained at different values of r. It also shows that, even when rigid local objects are rotationally (and translationally) disordered, the PDF still yields the intraobject structure, information that is lost in a crystallographic measurement in such a case.

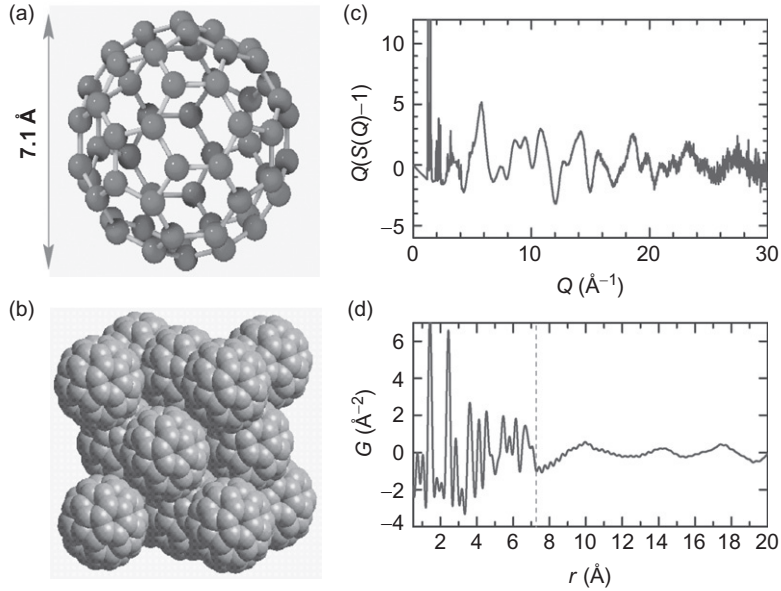

FIGURE 1.4 (a) The structure of a single C_{60} molecule. (b) The f.c.c arrangement of C_{60} balls in solid C_{60}. (c) Room temperature neutron powder diffraction data from a sample of solid C_{60} at room temperature. Note the pronounced diffuse scattering. The Bragg peaks from the f.c.c. arrangement of the balls are evident at very low Q. (d) Fourier transform of the data in (c) showing the PDF, $G(r)$, of solid C_{60}. The sharp features at low-r are the intraball C–C correlations. Above 7.1 Å only, interball correlations are present which are very weak because the balls are spinning.

1.2.3. Relevance to the Properties I: Bulk Nanostructured Thermoelectrics

When a temperature gradient is placed across a thermoelectric material, a voltage is induced. When built into devices, such materials can be used to obtain electricity from waste heat streams such as vehicle exhausts and industrial processes. The device can also be run in reverse. An applied voltage results in a temperature gradient across the material, which can be utilized for solid-state refrigeration. To be commercially viable, the devices need to have higher efficiencies, but how to improve the thermoelectric figure of merit of such materials in a cost-effective way (Nolas *et al*., 2006)? The dimensionless thermoelectric figure of merit, $ZT = \sigma S^2 T/\kappa$ where T is the operating temperature of the device, S is the thermopower, and σ and κ are the electrical and thermal conductivities of the material, respectively. It is notoriously difficult to raise the ZT of a material because σ and κ are related; if you raise σ, you tend also to raise κ, canceling the effect in the figure of merit, as one is in the numerator and the other is in the denominator. A strategy has been to

seek nanostructured materials where the pathways for electron transport are not disrupted, but nonetheless, there is strong phonon scattering from a nanostructure, and therefore a small κ, so-called electron crystal phonon glass materials (Slack, 1995). These are often materials with complicated open structures such as skutterudites and clathrates. It was somewhat of a surprise to find similarly low thermal conductivities in materials related to the simple binary compound, lead telluride in the lightly alloyed, so-called LAST material (Hsu *et al.*, 2004) where antimony and tin are doped into PbTe. It is now becoming apparent that nanophase separation and nanoscale precipitates embedded in the host lattice are providing the strong phonon scattering which, combined with the other good properties of the material, make for record breaking *ZT* values. For example, the *ZT* of one of these materials was found to reach 1.7 at 700 K, compared to the highest observed *ZT* of only 0.84 for PbTe at 648 K (Hsu *et al.*, 2004), a surprisingly large enhancement in *ZT* for the addition of just 10% per formula unit of silver and antimony ions.

High-resolution transmission electron microscopy (HRTEM) images from these materials indicate the presence of nanosized domains of a Ag–Sb-rich phase endotaxially embedded in the matrix (Quarez *et al.*, 2005). The HRTEM images show the clusters are randomly distributed through the matrix, are not long-range ordered, and strain the lattice. Because the endotaxial nanoparticles are random, their composition and size could not be studied crystallographically, but from modeling the PDF data, their structure and composition were elucidated (Lin *et al.*, 2005). Fits of phase-separated models to the PDFs obtained from alloys of different composition are shown in Fig. 1.5, and the resulting structural models are shown in Fig. 1.6. Similar results were obtained where, instead of the cation site, the anion Te site was alloyed, this time with sulfur (Lin *et al.*, 2009). This system is known to phase-separate, but very close to the composition where bulk phase separation sets in a PDF analysis coupled with crystallography and TEM showed that, although bulk phase separation is suppressed, there were local nanodomains of partially phase-separated material (Lin *et al.*, 2009).

1.2.4. Relevance to the Properties II: CMR Manganites

The CMR phenomenon is related to a magnetic field-induced insulator-to-metal transition. It turns out that hole localization due to polaron formation is an important component, and the PDF method played a major role in elucidating this mechanism. The key to the problem is the coupling of electrons to the lattice via a Jahn–Teller (JT) distortion (Goodenough *et al.*, 1961): locally, MnO_6 octahedra elongate to break an electronic degeneracy. In the $La_{1-x}Sr_xMnO_3$ system, the undoped, insulating compound, $LaMnO_3$, is JT distorted. This is clearly seen in the local structure (Fig. 1.7)

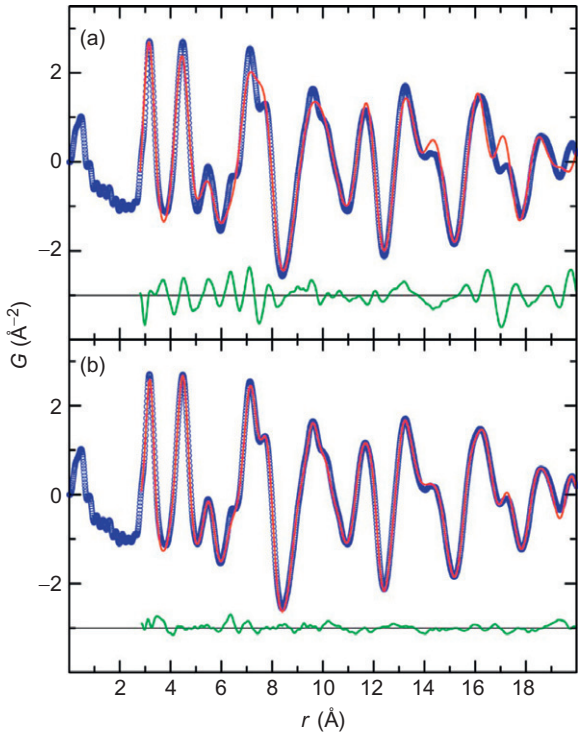

FIGURE 1.5 PDFs measured from the high-performance thermoelectric material $AgPb_6SbTe_8$ (open circles). In (a), the PDF calculated from a homogeneous model where there is no phase separation assumed is shown as the solid line, with a difference curve offset below. In (b), the PDF of the best fit model assuming nanophase separation is shown. The two-phase models in the latter case resulted in quantitative structural parameters from the nanophase (Lin *et al.*, 2005).

(Proffen *et al.*, 1999) as the first Mn–O peak in the PDF at $r \sim 2.0$ Å being split into two components.[3]

Because the JT-distorted octahedra have long-range orientational order, the "distortions" are also seen in the average structure. The crystal structure indicates that the JT distortion is quickly reduced as the valence of Mn is increased from 3+ toward 4+ by replacing La^{3+} with Sr^{2+}. By the time the MI transition occurs at $x = 0.16$, the JT distortion in the global structure is completely gone. However, it is still evident in the local structure as long Mn—O bonds are evident in the PDF (Fig. 1.8) (Louca and Egami, 1997). The distortion disappears in the average structure because the distorted octahedra become orientationally disordered with the long axes lying along

3. It appears as a negative peak because of the negative neutron scattering length of Mn. The reason why will be clear after studying the detailed definition of the PDF in Chapter 3.

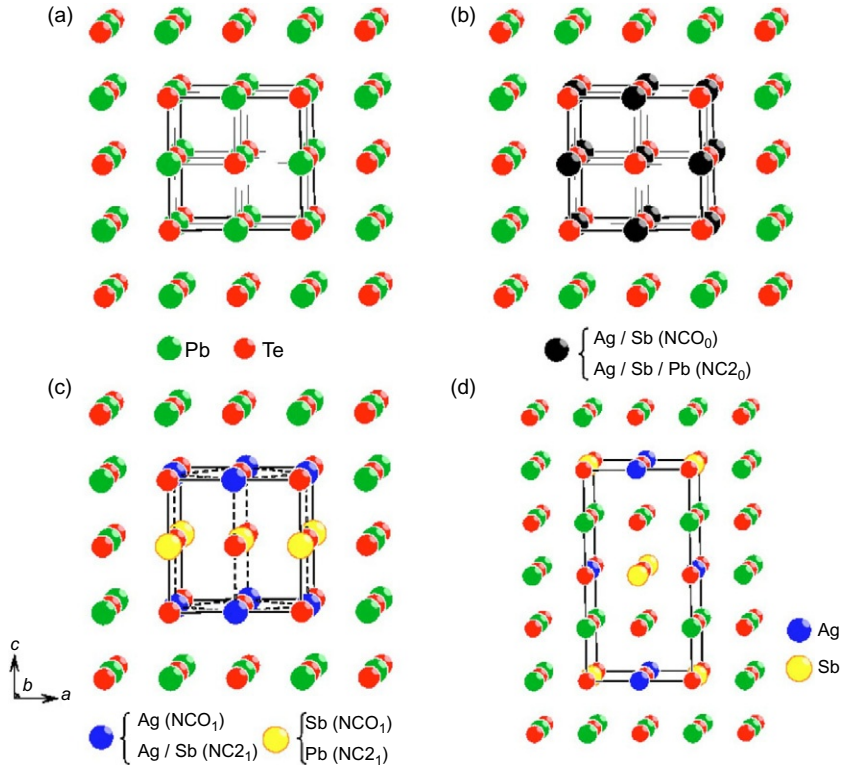

FIGURE 1.6 Models of the different endotaxial nanophases that were modeled as shown in Fig. 1.5. These could not be studied crystallographically because they are distributed randomly through the lattice but yield to a PDF analysis. They are crucial to the properties of this material.

x, y, and z directions with equal probability. The importance of this electron–lattice interaction to the CMR phenomenon itself was also demonstrated from a PDF measurement. An anomalous broadening at the MI transition of the PDF peaks associated with the Mn–O_6 octahedra was interpreted as electron localization and polaron formation (Fig. 1.9) with the appearance locally of JT lattice distortions (Billinge *et al.*, 1996).

1.2.5. Dynamical Disorder and Symmetry Lowering in Silica

Silica (SiO_2) is the basis of window glass. It also comes in crystalline forms, the best known being quartz. The silicon atoms are tetrahedrally coordinated with oxygen. As each oxygen has two silicon neighbors, this forms into a continuous tetrahedral network. At low temperature, silica forms the so-called

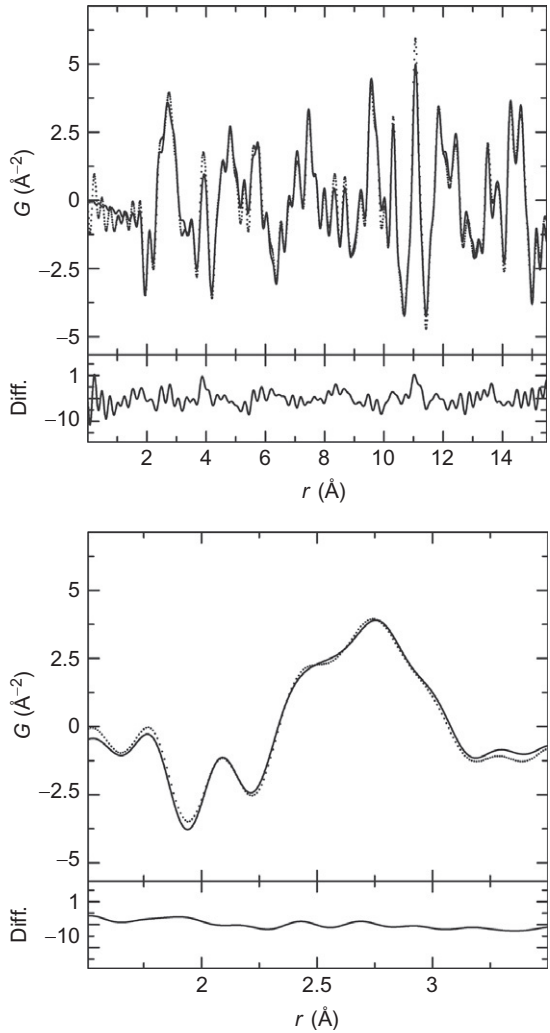

FIGURE 1.7 PDF of $LaMnO_3$ from neutron powder diffraction data collected at 10 K on the SEPD instrument at IPNS (dots). Note the first (negative) peak around $r = 2$ Å coming from Mn–O pairs is split into a well-resolved doublet showing the existence of short and long Mn—O bonds. This directly shows the Jahn–Teller distorted MnO_6 octahedra and is shown on an expanded scale in the lower panel. The solid line is the PDF calculated from a refined model of the structure using PDFFIT. The difference curve is shown below (Proffen *et al.*, 1999).

α-quartz phase; on heating, this transforms into β-quartz, then HP-tridymite, and then β-cristobalite before melting at 1727 °C. These are all phases with slightly different crystal structures. If cooled quickly or under pressure, yet more phases appear including, on fast cooling, the glass phase. These phase transitions have recently been studied using total scattering techniques

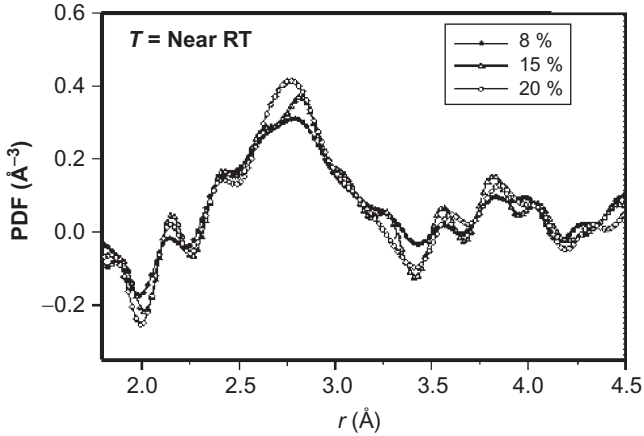

FIGURE 1.8 PDF from $La_{1-x}Sr_xMnO_3$ with different values of x showing the persistence of the Mn—O long bond around 2.15 Å in the PDF despite the fact that the crystal structure indicates that the Jahn–Teller distortion has disappeared on average (Louca and Egami, 1997).

which revealed unique information (Keen, 1998; Keen and Dove, 1999; Tucker *et al*., 2000a,b). These studies show that the old ideas of displacive versus order–disorder transitions do not capture the whole truth of what is happening, at least in the transitions in these materials. This became clear by studying the average structure and the local structure at the same time using total scattering methods. For example, in the phase transition in quartz at $T = 846$ K, the Si—O bond length changes smoothly from 1.61 Å at low temperature to 1.586 Å above the transition. These bond lengths were obtained from the average structure using Rietveld refinement of neutron powder diffraction data. However, PDFs obtained from these same data showed that, over the same temperature range, the local Si—O bond evolved from 1.61 Å at low temperature to 1.62 Å at 1000 K. This modest increase in bond length was a result of the natural thermal expansion of the SiO_4 octahedra and in sharp contrast to the behavior of the average bond length. This is shown in Fig. 1.10 that shows the Si—O bond length obtained from the PDF and from Rietveld on the same plot (Tucker *et al*., 2000a,b). Both results were obtained from the same sample and, indeed, from the same sets of data. The reason for this observation is that, in the high-temperature phase, the tetrahedra are dynamically rotating in such a way that the oxygen atom between the tetrahedra can rotate about the average bond axis. Consequently, the Si—O—Si bond in the average structure is straight, and the Si—O bond is therefore given by half the Si–Si distance. In reality, the local bond angle for the Si—O—Si bond remains closer to 150°, and the oxygen atom rotates around the average bond. This is illustrated in the bottom of Fig. 1.10 (Tucker *et al*., 2000a).

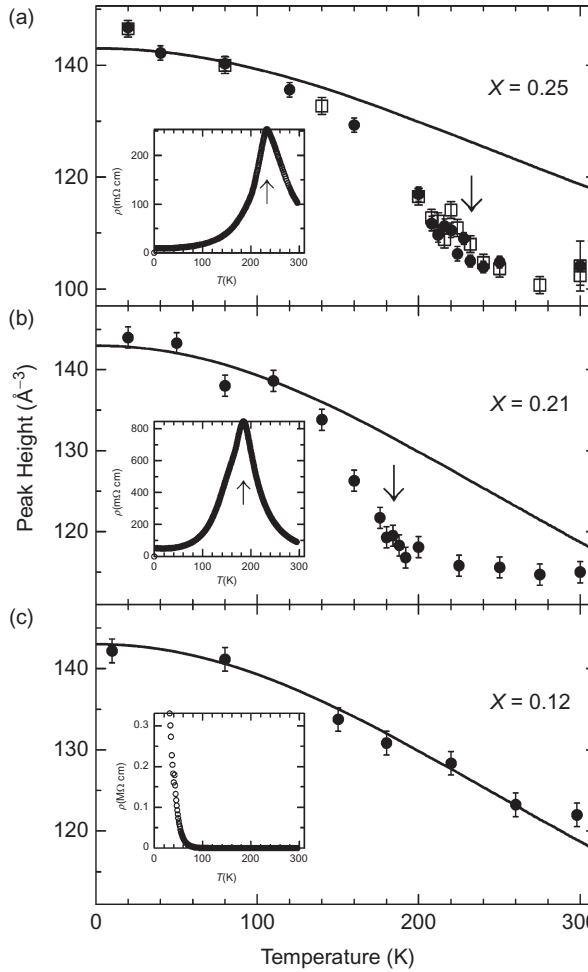

FIGURE 1.9 PDF peak height versus temperature of the PDF peak at $r = 2.75$ Å in $La_{1-x}Ca_xMnO_3$. The solid lines show the expected decrease in peak height from increasing PDF peak width due to enhanced thermal motion at higher temperature. In the two samples which have a MI transition (indicated by an arrow), there is an anomalous drop off in peak height indicating additional nonthermal disorder which is coming from polaron formation at high temperature. This PDF evidence was some of the most compelling supporting the view that polaron formation and electron–lattice interactions were important for understanding these CMR materials (Billinge *et al*., 1996).

1.2.6. Chemical Short-Range Order: β-Na_3BiO_4

β-Na_3BiO_4 presents an example of the kind of structural complexity that is becoming more widespread, and sought after, in modern materials (Vensky *et al*., 2005) and which requires techniques that go beyond crystallography, such as PDF, properly to characterize. Recently synthesized for the first time

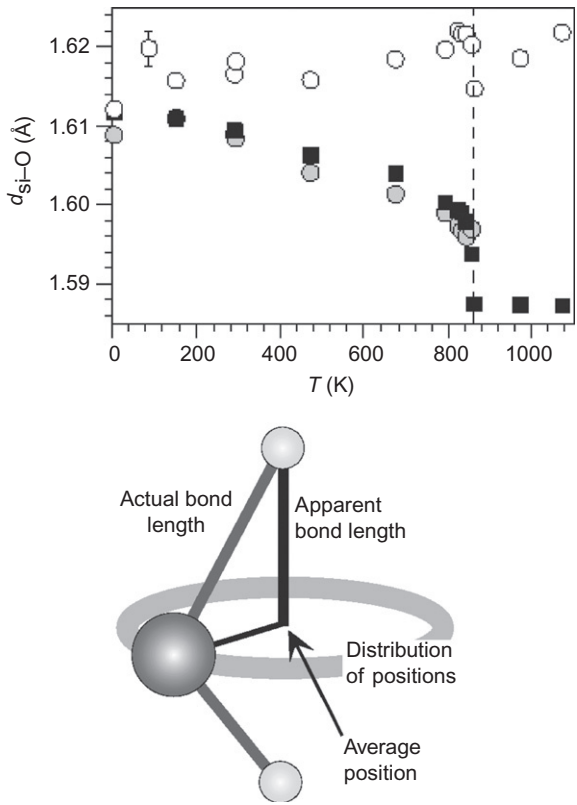

FIGURE 1.10 Si—O bond length in α-quartz versus temperature determined from the average structure and from the PDF. The actual bond length increases modestly due to thermal expansion up to 1000 K as seen from the PDF measurement (○). The anomalous shortening of the Si—O bond evident in the average structure (■) comes about because of thermally induced rotations of the Si-O_4 tetrahedra about the Si–Si axis as shown in the lower part of the figure (Tucker *et al*., 2000a, 2002).

and studied structurally using single crystal crystallography, it has layers in its rhombohedral structure containing Bi and Na in a 1:3 ratio with the metals disordered over the anion sites. However, the PDF revealed a more complex and interesting behavior, as evident in Fig. 1.11. As expected, fits of the disordered crystallographic model worked rather well at fitting the high-*r* region of the PDF (Fig. 1.11, top panel), but this model gave two clear peaks at ~2.5–4.8 Å that were not there in the data. On the other hand, a model with short-range-ordered Bi and Na similar to the low temperature α-Na_3BiO_4 polymorph fits this region perfectly (Fig. 1.11, lower panel), though extending this ordered model to high-*r* in the PDF fits is clearly disastrous as evident in the figure. This is a clear illustration that the PDF contains additional

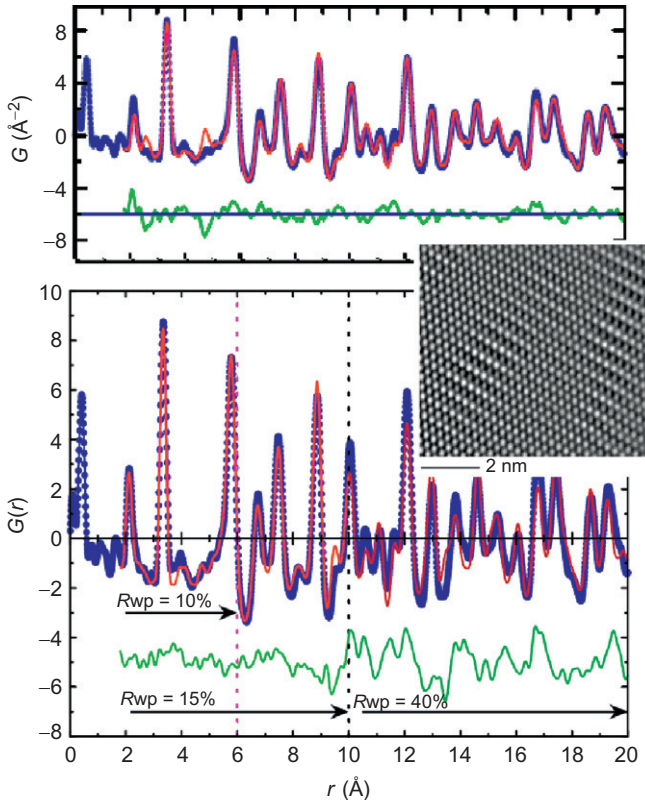

FIGURE 1.11 PDFs of β-Na_3BiO_4 (open circles). Solid curves are the best fit PDFs from models with difference curves offset below. In the low-r region below 6 Å, the model of chemically ordered Na and Bi, shown in the lower panel, fits the measured PDF better. At high-r (and crystallographically), the model of disordered Na and Bi fits much better. The layering takes place in specific crystallographic layers. The correct model has local chemical ordering with antiphase boundaries. A high-resolution transmission electron microscope image (inset) graphically confirms this (Vensky *et al*., 2005).

information than the Bragg diffraction which is insensitive to this short-range order. It is straightforward to reconcile the local and average structure in this case. Because the Na and Bi reside in crystallographic layers in the structure, you can have local Bi and Na ordering that does not propagate over long range if there are locally ordered domains, randomly distributed through the lattice, separated by antiphase domain walls. On average, this will result in disorder over the periodically averaged anion sites as seen crystallographically. This is indeed the case in this material as these domains can be seen directly in HRTEM images as shown in the figure. The PDF sees the local structure at low-r and the average structure at high-r.

1.3. RESOURCES FOR LEARNING TOTAL SCATTERING AND PDF METHODS

A number of resources are available to help people get started using PDF and total scattering methods beyond reading references cited in this book. At the end of the chapter, we present a list of review articles and book chapters that give more pointers to the beginner than we can include in this book. There are also online tutorials in diffraction and PDF methods present at http://www.lks.physik.uni-erlangen.de/diffraction/ to help learn basic diffraction theory and understand the origin of diffuse scattering (Proffen *et al.*, 2001). One of the best ways to get started is to download some of the open source software available for PDF analysis and modeling. It often comes very well documented and with tutorial examples, including data to do these tutorials for yourself. There is no better way to learn than to do. The software mostly comes with extensive documentation including tutorial examples to give new users experience in carrying out analyses. Good resources are the Diffpy Web site (www.diffpy.org) which contains the Billinge-group software (PDFgui, PDFfit, SrFit, and SrReal). Among these programs, PDFgui is the most mature and probably the best place to start. There is an active user community who share tips and tricks, and go to find solutions to problems, at the Google-group "diffpy-users" (bug reports and feature requests should be sent to the diffpy-dev Google group). The DISCUS suite of programs, available from sourceforge, is also particularly well documented, with its own "cookbook" of examples published (Neder and Proffen, 2008). We will share a more complete list of available software later in the book, but various other programs for total scattering and PDF analysis are available and appear over time and many of them can be a good place to start your PDF journey. From time to time, PDF and total scattering workshops are organized, for example, at major national meetings such as the annual meeting of the American Crystallographic Association. Finally, as the method grows in popularity, X-ray and neutron beamlines dedicated to, or optimized for, PDF analysis are popping up at various X-ray and neutron sources. The instruments scientists at these beamlines are one of the best resources for getting started using the PDF method. They are generally highly knowledgeable and eager to help people who have interesting scientific problems for PDF analysis but lack the knowledge to do the experiments for themselves. The best approach is to send them an e-mail with a brief description of the experiment you would like to do, and they can advise how to proceed. At the time of writing, such beamlines include 11IDB and 11IDC at the advanced photon source at Argonne National Laboratory in the USA, X17A at NSLS and XPD at NSLS-II at Brookhaven National Laboratory, NPDF at the Lujan Center of the Los Alamos National Laboratory, NOMAD at the Spallation Neutron Source at Oak Ridge National Laboratory, all in the US, ID11 and ID15 at the ESRF in Grenoble, France, GEM and NIMROD at ISIS, and a new X-ray PDF beamline under

construction at Diamond, both at the Rutherford Appleton Laboratory in the UK and BL14B1 at Spring8 in Japan. The PETRA-III facility in Hamburg is also commissioning a beamline suitable for PDF studies, with others likely to follow elsewhere.

REFERENCES

Billinge, S.J.L. (2010) *Physics*, **3**, 25.

Billinge, S.J.L. & Levin, I. (2007) *Science*, **316**, 561.

Billinge, S.J.L., DiFrancesco, R.G., Kwei, G.H., Neumeier, J.J. & Thompson, J.D. (1996) *Phys. Rev. Lett.*, **77**, 715.

Egami, T. & Aur, S. (1987) *J. Non-Cryst. Solids*, **89**, 60.

Egami, T., Dmowaski, W., He, Y. & Schwarz, R. (1998) *Metall. Mater. Trans.*, **29A**, 1805.

Eshelby, J.D. (1956) F. Seitz & D. Turnbull (Eds.), *Solid State Physics*Vol. 3. (p. 79). New York: Academic Press.

Goodenough, J.B., Wold, A., Arnott, R.J. & Menyuk, N. (1961) *Phys. Rev.*, **124**, 373.

Hsu, K.F., Loo, S., Guo, F., Chen, W., Dyck, J.S., Uher, C., Hogan, T., Polychroniadis, E.K., Mercouri, G. & Kanatzidis, M.G. (2004) *Science*, **303**, 818.

Jeong, I.-K., Mohiuddin-jacobs, F., Petkov, V. & Billinge, S.J.L. (2001) *Phys. Rev. B*, **63**, 205202.

Juhás, P., Cherba, D.M., Duxbury, P.M., Punch, W.F. & Billinge, S.J.L. (2006) *Nature*, **440**, 655.

Keen, D.A. (1998) S.J.L. Billinge & M.F. Thorpe (Eds.), *Local Structure from Diffraction* (p. 101). New York: Plenum Press.

Keen, D.A. & Dove, M.T. (1999) *J. Phys. Condens. Matter*, **11**, 9263.

Lin, H., Božin, E.S., Billinge, S.J.L., Quarez, E. & Kanatzidis, M.G. (2005) *Phys. Rev. B*, **72**, 174113.

Lin, H., Božin, E.S., Billinge, S.J.L., Androulakis, J., Lin, C.H. & Kanatzidis, M.G. (2009) *Phys. Rev. B*, **80**, art. no. 045204.

Louca, D. & Egami, T. (1997) *Phys. Rev. B*, **56**, R8475.

Mikkelson, J.C. & Boyce, J.B. (1982) *Phys. Rev. Lett.*, **49**, 1412.

Neder, R.B. & Proffen, Th. (2008) *Diffuse Scattering and Defect Structure Simulations: A Cook Book Using the Program DISCUS*. Oxford: Oxford University Press.

Nolas, G.S., Poon, J. & Kanatzidis, M. (2006) *MRS Bull.*, **31**, 199.

Petkov, V., Jeong, I.-K., Chung, J.S., Thorpe, M.F., Kycia, S. & Billinge, S.J.L. (1999) *Phys. Rev. Lett.*, **83**, 4089.

Proffen, T., DiFrancesco, R.G., Billinge, S.J.L., Brosha, E.L. & Kwei, G.H. (1999) *Phys. Rev. B*, **60**, 9973.

Proffen, T., Neder, R.B. & Billinge, S.J.L. (2001) *J. Appl. Crystallogr.*, **34**, 767.

Quarez, E., Hsu, K.F., Pcionek, P., Frangis, N., Polychroniadis, E.K., Kanatzidis, M.G. & Amer, J. (2005) *Chem. Soc.*, **127**, 9177.

Slack, G.A. (1995) D.M. Rowe (Ed.), *CRC Handbook of Thermoelectrics*. Boca Raton, FL: Chemical Rubber Ch. 34.

Tucker, M.G., Dove, M.T. & Keen, D.A. (2000a) *J. Phys. Condens. Matter*, **12**, L425.

Tucker, M.G., Dove, M.T. & Keen, D.A. (2000b) *J. Phys. Condens. Matter*, **12**, L723.

Tucker, M.G., Dove, M.T. & Keen, D.A. (2002) M.F. Thorpe (Ed.), *From Semiconductors to Proteins: Beyond the Average Structure* (p. 85). New York: Kluwer/Plenum.

Vensky, S., Kienle, L., Dinnebier, R.E., Masadeh, A.S., Billing, S.J.L. & Jansen, M. (2005) *Z. Kristallogr.*, **220**, 231.

The following books and review articles give traditional introductions to the PDF technique as applied to noncrystalline materials using conventional sources. They are useful resources, as the mathematics and definitions do not change between amorphous and crystalline materials. For completeness, all the important relations are reproduced in later chapters of this book. Apart from Billinge and Thorpe (1998) which contains an overview of a number of different techniques for studying local structure, these books are quite out of date regarding X-ray sources, experiments, and data modeling.

Barnes, A.C., Fischer, H.E. & Salmon, P.S. (2003) *J. Phys. IV*, **111**, 59.
Billinge, S.J.L. & Thorpe, M.F. (1998) *Local Structure from Diffraction*. New York: Plenum.
Klug, H.P. & Alexander, L.E. (1974) *X-ray Diffraction Procedures* (2nd Edition). New York: Wiley.
Wagner, C.N.J. (1978) *J. Non-Cryst. Solids*, **31**, 1.
Warren, B.E. (1990) *X-ray Diffraction*. New York: Dover.
Waseda, Y. (1980) *The Structure of Non-crystalline Materials*. New York: McGraw-Hill.
Wright, A.C. (1985) *J. Non-Cryst. Solids*, **76**, 187.

The following, book chapters and review articles cover more recent applications of the PDF technique to nanostructured materials including disordered crystals.

Billinge, S.J.L. & Kanatzidis, M.G. (2004) *Chem. Commun.*, 749.
Billinge, S.J.L. (2008a) *J. Solid State Chem.*, **181**, 1698.
Billinge, S.J.L. (2008b) R.E. Dinnebier & S.J.L. Billinge (Eds.), *Powder Diffraction: Theory and Practice* (p. 464). London, England: Royal Society of Chemistry Ch. 16.
Božin, E.S., Juhás, P. & Billinge, S.J.L. (2012) C. Lamberti (Ed.), *Characterization of Semiconductor Heterostructures and Nanostructures*. (2nd Edition). Amsterdam: Elsevier.
Neder, R.B. & Proffen, Th. (2008) *Diffuse Scattering and Defect Structure Simulations: A Cook Book Using the Program DISCUS*. Oxford: Oxford University Press.
Proffen, T., Billinge, S.J.L., Egami, T. & Louca, D. (2003) *Z. Kristallogr.*, **218**, 132.
Young, C.A. & Goodwin, A.L. (2011) *J. Mater. Chem.*, **21**, 6464.